Applied Physics Letters

Tuning carrier density at complex oxide interface with metallic overlayer

Cite as: Appl. Phys. Lett. **108**, 231603 (2016); https://doi.org/10.1063/1.4953586
Submitted: 21 March 2016 . Accepted: 27 May 2016 . Published Online: 08 June 2016

Y. Zhou, Y. J. Shi, S. W. Jiang, F. J. Yue, P. Wang, H. F. Ding, and D. Wu

View Online Export Citation CrossMark

ARTICLES YOU MAY BE INTERESTED IN

Patterning the two dimensional electron gas at the $LaAlO_3/SrTiO_3$ interface by structured Al capping
Applied Physics Letters **110**, 141603 (2017); https://doi.org/10.1063/1.4979784

Spin rectification induced by spin Hall magnetoresistance at room temperature
Applied Physics Letters **109**, 112406 (2016); https://doi.org/10.1063/1.4962895

Tuning the carrier density of $LaAlO_3/SrTiO_3$ interfaces by capping $La_{1-x}Sr_xMnO_3$
Applied Physics Letters **102**, 071605 (2013); https://doi.org/10.1063/1.4793576

Lock-in Amplifiers up to 600 MHz
Watch

AIP Publishing

© 2016 Author(s).

Tuning carrier density at complex oxide interface with metallic overlayer

Y. Zhou,[1] Y. J. Shi,[1] S. W. Jiang,[1] F. J. Yue,[1] P. Wang,[1] H. F. Ding,[1,2] and D. Wu[1,2,a)]
[1]*National Laboratory of Solid State Microstructures and Department of Physics, Nanjing University, 22 Hankou Road, Nanjing 210093, People's Republic of China*
[2]*Collaborative Innovation Center of Advanced Microstructures, Nanjing University, 22 Hankou Road, Nanjing 210093, People's Republic of China*

(Received 21 March 2016; accepted 27 May 2016; published online 8 June 2016)

We have systematically investigated the electronic transport properties of the $LaAlO_3/SrTiO_3$ interfaces with several different metal capping layers. The sheet carrier density can be tuned in a wide range by the metallic overlayer without changing the carrier mobility. The sheet carrier density variation is found to be linearly dependent on the size of metal work function. This behavior is explained by the mechanism of the charge transfer between the oxide interface and the metal overlayer across the $LaAlO_3$ layer. Our results confirm the existence of a built-in electric field in $LaAlO_3$ film with an estimated value of 67.7 eV/Å. Since the metallic overlayer is essential for devices, the present phenomena must be considered for future applications. *Published by AIP Publishing.*
[http://dx.doi.org/10.1063/1.4953586]

High mobility quasi-two-dimensional electron gas (q-2DEG) at complex oxide heterointerfaces has attracted a great deal of interest due to their rich physics and potential applications in next-generation microelectronics.[1] The q-2DEG formed at the interface between the two band insulators $LaAlO_3$ (LAO) and $SrTiO_3$ (STO) is a prominent example.[2] It has been discovered that at low temperature, the LAO/STO interface shows a variety of electronic phases such as ferromagnetism,[3] superconductivity,[4] even coexistence of ferromagnetism and superconductivity.[5,6] The LAO/STO interface has been demonstrated to be a promising platform to realize field-effect transistor,[7,8] polar molecule sensors,[9] nano-photodetectors,[10] and even spintronic devices.[11,12]

The electric and magnetic properties of the LAO/STO interface are sensitive to the sheet carrier concentration n_{sheet}. The sheet carrier concentration was initially controlled by the oxygen pressure during the LAO layer growth, where the oxygen vacancies act as electron donors.[3] Modulation of n_{sheet} has also been obtained in a field effect transistor geometry device, where an electric field is applied between the interface and a metal[13] or the ferroelectric[14] gate electrode. The transfer of electrons from the LAO surface to the interface to overcome the electrostatic potential divergence built by the polar field in LAO layer, known as the charge reconstruction model, is believed to be one of the origins to the conductive interface.[15] This model represents that the electronic states of the LAO surface are closely related to the interface conductivity. Therefore, attempts to control n_{sheet} through manipulating the LAO surface have been carried out in several approaches. For example, the adsorbing polar molecules,[9] the writing of surface charge by atomic force microscopy tip,[8] and the capping of nanoparticles and polar materials on LAO surface are employed to alter n_{sheet}.[16,17] Considering that a metallic overlayer can significantly influence the surface electronic states of an oxide material,[18] n_{sheet} at LAO/STO interface should also be strongly modified by a metallic contact.[19] However, this issue has not been addressed experimentally.

To develop practical devices, the integration of the metallic contacts with the oxide interface is essential. For instance, a metallic electrode on top of the LAO layer in the field effect transistor device is indispensable.[13,20,21] The tunneling injection from a ferromagnetic metal through LAO into LAO/STO interface is a general approach for spin injection in spintronic devices.[11] The impact of the metallic overlayers on the interface properties needs to be considered accordingly. Here, we report a systematically study on the electronic transport properties of LAO/STO interface with a variety of metallic overlayers. The sheet carrier concentration can be modified in a wide range by the metallic overlayer without changing the carrier mobility. The built-in potential across the LAO layer as a correction is needed for different metallic electrodes and our newly estimated value is 67.7 eV/Å.

A 5-nm-thick amorphous LAO (a-LAO) film was grown on a TiO_2-terminated STO (001) substrate by pulsed laser deposition (PLD) with a shadow mask to define a proper shape at room temperature at the oxygen pressure of 1×10^{-1} Torr. After removing the shadow mask, another LAO film was epitaxially grown on the sample by PLD at 750 °C and the oxygen pressure of 5×10^{-5} Torr. The detailed growth process and characterization of the epitaxial LAO film has been described in detail in our previous report.[22] The thickness of the epitaxial grown LAO layer was 5 unit cell (u.c.) and monitored by *in situ* reflection high energy electron diffraction. The sample was annealed at 550 °C under atmospheric oxygen pressure for 4 h to remove the oxygen vacancies in LAO. Figure 1(a) shows the atomic force microscopy (AFM) image of the 5 u.c. LAO film on STO. The atomically flat terraces and 1 u.c. step height suggest that the LAO film is continuously formed. After the transport measurements on the LAO/STO interface, a 20-nm-thick metallic top electrode was *ex-situ* evaporated on the LAO surface by electron beam evaporation through a shadow mask to define a proper

a)Electronic mail: dwu@nju.edu.cn

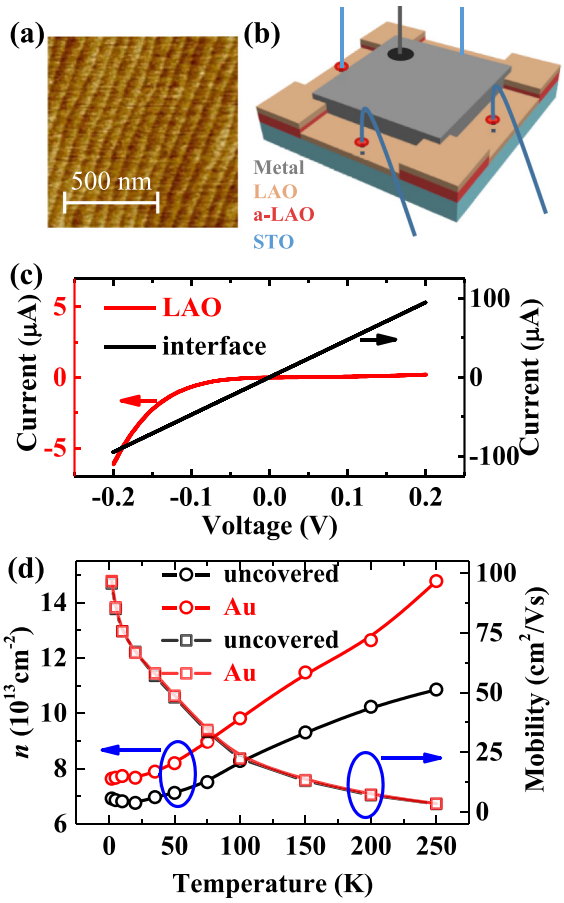

FIG. 1. Schematic and transport measurement of metal/LAO/STO devices. (a) AFM image of the 5 u.c. LAO layer on STO. A clear step-and-terrace surface is observed. (b) Sketch of the samples and the contact configurations using silver paint (black circle) and wire bonder (red circle). a-LAO indicates the amorphous LAO layer. (c) *I-V* curves of LAO/STO interface and across LAO layer. (d) Temperature dependence of the carrier density and mobility of the LAO/STO interface before and after depositing gold, respectively.

shape. Finally, the conductive LAO/STO interface was patterned into a cross geometry with a metallic top contact, as schematically shown in Figure 1(b). Four Al wires were connected to the LAO/STO interface by ultrasonic bonding in four-probe van der Pauw geometry. The top metallic layer was connected by a silver paint without contacting the LAO layer.

Figure 1(c) shows the typical current-voltage (*I-V*) curves measured on the LAO/STO interface and between a gold top electrode and the LAO/STO interface at 2 K. A linear *I-V* characteristic is observed for the interface, indicating that Ohmic contacts are achieved between Al wires and the interface by wire-bonding. In contrast, a highly rectifying *I-V* curve across the LAO layer is obtained, directly suggesting that the LAO layer forms an asymmetric tunneling barrier. Here, a positive bias voltage means that the voltage of the metallic electrode is higher than that of the LAO/STO interface. Importantly, the resistance of the interface is several orders of magnitude smaller than that of the LAO tunneling barrier at low bias voltage region. Therefore, when n_{sheet} of the LAO/STO interface is measured by the Hall effect at low current, the current tunneling to the gold electrode can be neglected.

n_{sheet} of the LAO/STO interface is sensitive to the growth condition. To reduce the uncertainty caused by the sample-to-sample variation, we compare n_{sheet} for the same sample before and after the deposition of the metallic overlayer unless otherwise specified. Figure 1(d) shows n_{sheet} of the LAO/STO interface with and without gold overlayer as a function of the temperature. n_{sheet} is about $1.09 \times 10^{14}\,cm^{-2}$ without Au overlayer at 250 K, which is consistent with the previously reported areal carrier density of the interface grown under the similar condition.[23] After the gold layer deposition, n_{sheet} increases ~40% to $1.48 \times 10^{14}\,cm^{-2}$ with the same given temperature. n_{sheet} gradually decreases as decreasing temperature for both samples and n_{sheet} of the interface with gold overlayer is always smaller than that of the interface with gold overlayer in all temperature range. Unlike the gate electric field and polar molecular adsorption changing n_{sheet} and the mobility simultaneously,[9,20] the Hall mobility remains the same after the deposition of gold in all temperature range, as shown in Figure 1(d). Although the mobility of our samples is relatively low, it can still be modulated in a wide range by the gate voltage (see the supplementary material).[24] Besides Au, we have extended the investigation to a variety of the metallic overlayers: Al, Ti, Co, and Pt. We found that n_{sheet} can be modified in a wide range by these metallic overlayers. The results of the change of n_{sheet}, Δn, after the deposition of the overlayers measured at 2 K are summarized as a function of the work function in Figure 2. Unlike the adsorption of the polar molecules, which only increase the interface conductivity,[9] the metallic overlayer can increase or reduce n_{sheet} and thereby the corresponding conductivity. Moreover, Δn is comparable to that by conventional gate field tuning approach. Δn monotonically decreases as increasing the work function, indicating the strong correlation between the work function and n_{sheet}.

The mobile carriers in the LAO/STO interface have been suggested to be originated from the oxygen vacancies,[25–28] interface interdiffusion,[29] and electronic reconstruction.[15] In our experiments, the metal overlayers are grown at room temperature, and the LAO/STO interfaces are from the same piece of sample. The interface interdiffusion is expected to be the same for all samples. The redox reaction at the LAO/STO upon the deposition of metal may induce the oxygen vacancies.[26,27] We did a control experiment of depositing Al or Ti on an insulating LAO/STO interface. The interface is likely insulating, suggesting that the redox reaction mechanism may not play an important role

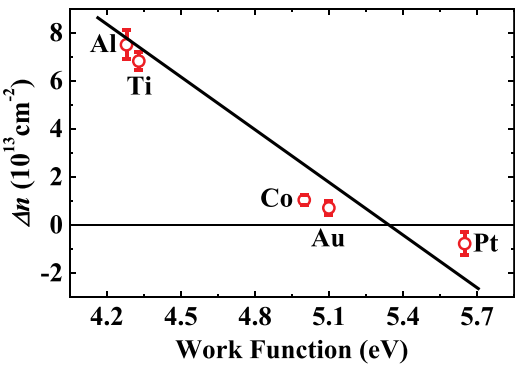

FIG. 2. The change in the carrier density of the LAO/STO interface after depositing Al, Ti, Co, Au, and Pt measured at 2 K, respectively. Straight line shows the fitting result using Eq. (1).

(see the supplementary material).[24] Moreover, the alteration of the oxygen vacancies and interface interdiffusion can significantly cause carrier mobility change. The observed unchanged carrier mobility [Figure 1(c)] strongly suggests that the oxygen vacancies and interface interdiffusion are not altered by the metal overlayer. Thus, these two mechanisms can be ruled out for the observed phenomena.

The variation of the carrier density induced by the metal overlayers can be understood by considering the charge transfer between the LAO/STO interface and the metal overlayer across the LAO layer. In the metal/LAO/q-2DEG tunnel junctions, the charge tunneling occurs due to the different work function $\Delta U = E_{\text{q-2DEG}} - E_{\text{m}}$ between the q-2DEG work function $E_{\text{q-2DEG}}$ and the metal work function E_{m} even without an external bias voltage, as schematically shown in Figure 3(a). The charges tunnel into or out the LAO/STO interface until the Fermi level of the two electrodes coincides, as shown in Figure 3(b). The amount of Δn can be quantified by treating the junction as a capacitor. $\Delta U/e$ acts as the bias voltage across the LAO layer, where e is the elementary electric charge. With the above analysis, we can obtain that

$$\Delta n = \frac{C\Delta U}{e^2 S} = \frac{\varepsilon_{\text{r}}}{4\pi k d_{\text{LAO}} e}(E_{\text{q-2DEG}} + E_{\text{d}} - E_{\text{m}}), \qquad (1)$$

where C is the junction capacitance, S is the junction area, $\varepsilon_{\text{r}} = 25$ is the dielectric constant of LAO, k is the Coulomb's constant, $d_{\text{LAO}} = 1.89$ nm is the thickness of the 5 u.c. LAO layer for the LAO lattice constant $a = 0.378$ nm, and E_{d} is the ionic build-in potential across LAO layer. Utilizing Eq. (1), we can well fit our measured data with only one parameter of $E_{\text{q-2DEG}} + E_{\text{d}}$ (Figure 2), confirming that Δn is indeed due to the work function difference induced charge transfer. In our measurement, Δn is obtained from the Hall measurement, i.e., only mobile charges are detected. The reproduced fitting suggests that the transferred charges are almost not trapped at the interface but contribute to the mobile carriers. Moreover, the fitting yields $E_{\text{q-2DEG}} + E_{\text{d}}$ to be 5.35 eV. Given that the Fermi level of the LAO/STO interface is about $\Delta E = 0.03$ eV higher than the conduction band minimum of STO and the electron affinity of STO E_{STO} is 4.1 eV,[30] we can obtain $E_{\text{q-2DEG}} = E_{\text{STO}} - \Delta E = 4.07$ eV (Figure 3(a)). Therefore, the ionic build-in potential across 5 u.c. LAO is $E_{\text{d}} = 5.35 - E_{\text{q-2DEG}} = 1.28$ eV. For the 5 u.c. thick LAO layer, the build-in electric field within LAO is estimated to be 67.7 eV/Å, which is smaller than the previous reported value of 80.1 eV/Å by studying the Zener tunneling effect across LAO layer[31] but larger than the 30 eV/Å measured by the cross sectional scanning tunneling microscopy.[30] For both previous measurements, a metal overlayer was deposited on the LAO layer. If $E_{\text{m}} > 5.35$ eV (<5.35 eV), charges tunnel from (to) the metal layer to (from) the LAO/STO interface, resulting in an enhancement (reduction) of the electric field in LAO. Therefore, E_{d} could be misestimated with a metallic overlayer. In fact, after considering the charge transfer effect, the build-in electric field is estimated to be 61.5 eV/Å in the Zener tunneling measurement,[31] in good agreement with our result.

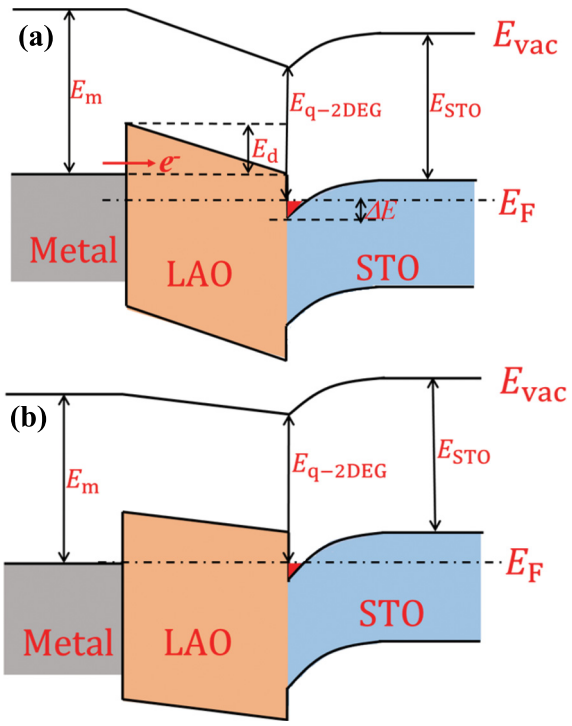

FIG. 3. Schematic band alignments of the metal/LAO/STO junction before (a) and after (b) the charge transfer.

In order to further understand the impact of the metal overlayer on the LAO/STO interface properties, we studied the tunneling effect between the interface and the different metallic overlayer. Again, to reduce the sample-to-sample variation, different metallic overlayers on the LAO/STO interface were fabricated. To achieve this, after 5 u.c. LAO epitaxially grown on STO, a 5-nm-thick amorphous LAO film was deposited at room temperature by PLD with a shadow mask to form a 300-μm-wide stripe, as schematically shown in Figure 4(a). About 300-μm-wide metallic strip defined by photolithography was fabricated perpendicular to the bare LAO stripe. Different metal overlayer was prepared in sequence. The optical micrograph of the sample layout is shown in Figure 4(b).

Figure 4(c) shows the I-V curves measured at 2 K between the LAO/STO interface and different metallic overlayers. The strong asymmetric behaviors strongly suggest that the LAO barrier is asymmetric. The current strongly depends on the type of the metallic overlayer. The higher the work function of the metallic overlayer is, the stronger the rectification behavior is observed, indicating that the built-in electric field in LAO points from the LAO/STO interface to the surface and the tunneling barrier height relies on the type of the metallic overlayer. In order to extract the barrier height ϕ for different junctions, the I-V curves for the positive bias voltage V are fitted by the direct tunneling model that is given by[32]

$$I = \frac{eS}{2\pi h}\left\{\left(\phi - \frac{eV}{2}\right)\exp\left[\frac{-4\pi d_{LAO}(2m^*)^{1/2}}{h}\left(\phi - \frac{eV}{2}\right)\right] - \left(\phi + \frac{eV}{2}\right)\exp\left[\frac{-4\pi d_{LAO}(2m^*)^{1/2}}{h}\left(\phi + \frac{eV}{2}\right)\right]\right\}, \qquad (2)$$

where h is the Planck constant, and m^* is the electron effective mass of the LAO/STO interface. The I-V curves can be

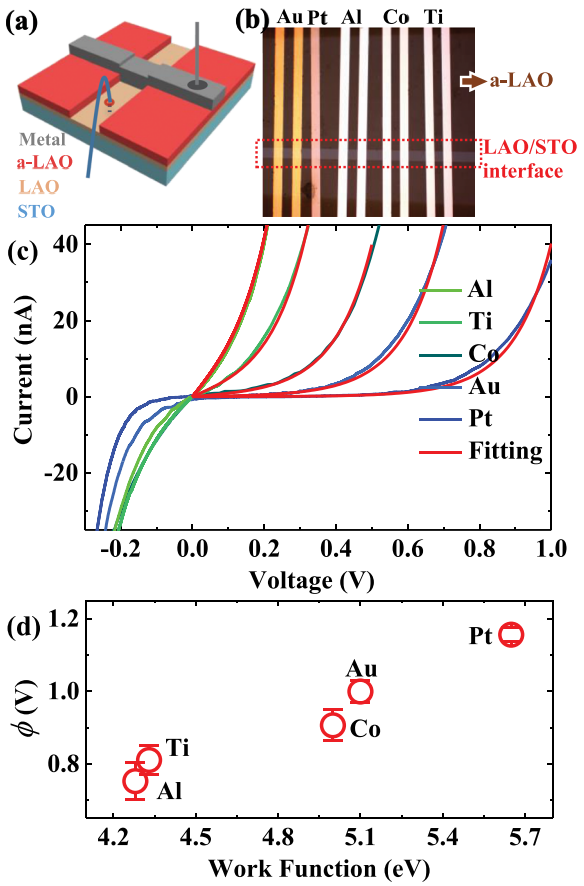

FIG. 4. The tunneling effect between the LAO/STO interface and the different metallic overlayer. (a) Sketch of the samples and the contact configurations using silver paint (black circle) and wire bonder (red circle). (b) Optical microscopy image of the tunneling junctions. (c) *I-V* curves between the LAO/STO interface and the different metal electrodes measured at 2 K. Red curves are the fitting results using Eq. (2). (d) Fitted ϕ between the LAO/STO interface and different metal overlayers against the corresponding metal work functions.

well fitted by Eq. (2) [red solid line in Figure 4(c)]. Because all junctions are based on the same conducting LAO/STO interface, m^* is considered to be the same for all junctions. The fittings give $m^* = 0.6m_0$ for all junctions, where m_0 is the free electron mass, consistent with the previous reported value.[31] For simplicity, here, a square tunneling barrier is used in Eq. (2), meaning that the obtained ϕ is the average barrier height.[33] Figure 4(d) plots ϕ obtained from the fitting against the corresponding metal work functions. Clearly, ϕ monotonically increases as increasing work function. The amount of charge transferring from the metal overlayer to the LAO/STO interface relies on the value of the metal work function. The transferred charge would build an additional electric field in LAO layer, leading to ϕ correlated with the work function of the metal overlayer.

In conclusion, we have demonstrated that the carrier density at the LAO/STO interface can be modified as large as $7.5 \times 10^{13}\,\mathrm{cm}^{-2}$ by a metallic overlayer without changing the carrier mobility, comparable to conventional gate field tuning approach. The results present direct evidence of the existence of the built-in electric field in the LAO layer with an estimated field of 67.7 eV/Å. Our findings provide a simple and powerful way in controlling this system. Since the metallic overlayer is essential for devices, the present phenomena must be considered for devices.

This work was supported by the National Basic Research Program of China (2013CB922103), the NSF of China (11222435 and 51471086), and the NSF of Jiangsu Province (BK20130054).

[1]H. Y. Hwang, Y. Iwasa, M. Kawasaki, B. Keimer, N. Nagaosa, and Y. Tokura, Nat. Mater. **11**, 103 (2012).
[2]A. Ohtomo and H. Y. Hwang, Nature **427**, 423 (2004).
[3]A. Brinkman, M. Huijben, M. van Zalk, J. Huijben, U. Zeitler, J. C. Maan, W. G. van der Wiel, G. Rijnders, D. H. Blank, and H. Hilgenkamp, Nat. Mater. **6**, 493 (2007).
[4]N. Reyren, S. Thiel, A. D. Caviglia, L. F. Kourkoutis, G. Hammerl, C. Richter, C. W. Schneider, T. Kopp, A.-S. Rüetschi, D. Jaccard, M. Gabay, D. A. Muller, J.-M. Triscone, and J. Mannhart, Science **317**, 1196 (2007).
[5]J. A. Bert, B. Kalisky, C. Bell, M. Kim, Y. Hikita, H. Y. Hwang, and K. A. Moler, Nat. Phys. **7**, 767 (2011).
[6]L. Li, C. Richter, J. Mannhart, and R. C. Ashoori, Nat. Phys. **7**, 762 (2011).
[7]S. Thiel, G. Hammerl, A. Schmehl, C. W. Schneider, and J. Mannhart, Science **313**, 1942 (2006).
[8]C. Cen, S. Thiel, G. Hammerl, C. W. Schneider, K. E. Andersen, C. S. Hellberg, J. Mannhart, and J. Levy, Nat. Mater. **7**, 298 (2008).
[9]Y. Xie, Y. Hikita, C. Bell, and H. Y. Hwang, Nat. Commun. **2**, 494 (2011).
[10]P. Irvin, Y. Ma, D. F. Bogorin, C. Cen, C. W. Bark, C. M. Folkman, C. Eom, and J. Levy, Nat. Photonics **4**, 849 (2010).
[11]N. Reyren, M. Bibes, E. Lesne, J.-M. George, C. Deranlot, S. Collin, A. Barthélémy, and H. Jaffrès, Phys. Rev. Lett. **108**, 186802 (2012).
[12]F. Bi, M. Huang, S. Ryu, H. Lee, C.-W. Bark, C.-B. Eom, P. Irvin, and J. Levy, Nat. Commun. **5**, 5019 (2014).
[13]B. Förg, C. Richter, and J. Mannhart, Appl. Phys. Lett. **100**, 053506 (2012).
[14]V. T. Tra, J.-W. Chen, P.-C. Huang, B.-C. Huang, Y. Cao, C.-H. Yeh, H.-J. Liu, E. A. Eliseev, A. N. Morozovska, J.-Y. Lin, Y.-C. Chen, M.-W. Chu, P.-W. Chiu, Y.-P. Chiu, L.-Q. Chen, C.-L. Wu, and Y.-H. Chu, Adv. Mater. **25**, 3357 (2013).
[15]N. Nakagawa, H. Y. Hwang, and D. A. Muller, Nat. Mater. **5**, 204 (2006).
[16]H. Kim, N. Y. Chan, J. Dai, and D.-W. Kim, Sci. Rep. **5**, 8531 (2015).
[17]K. Au, D. F. Li, N. Y. Chan, and J. Y. Dai, Adv. Mater. **24**, 2598 (2012).
[18]Y. F. Dong, Y. Y. Mi, Y. P. Feng, A. C. H. Huan, and S. J. Wang, Appl. Phys. Lett. **89**, 122115 (2006).
[19]R. Arras, V. G. Ruiz, W. E. Pickett, and R. Pentcheva, Phys. Rev. B **85**, 125404 (2012).
[20]M. Hosoda, Y. Hikita, H. Y. Hwang, and C. Bell, Appl. Phys. Lett. **103**, 103507 (2013).
[21]S. Wu, X. Luo, S. Turner, H. Peng, W. Lin, J. Ding, A. David, B. Wang, G. Van Tendeloo, J. Wang, and T. Wu, Phys. Rev. X **3**, 041027 (2013).
[22]Y. J. Shi, S. Wang, Y. Zhou, H. F. Ding, and D. Wu, Appl. Phys. Lett. **102**, 071605 (2013).
[23]G. Herranz, M. Basletić, M. Bibes, C. Carrétéro, E. Tafra, E. Jacquet, K. Bouzehouane, C. Deranlot, A. Hamzić, J.-M. Broto, A. Barthélémy, and A. Fert, Phys. Rev. Lett. **98**, 216803 (2007).
[24]See supplementary material at http://dx.doi.org/10.1063/1.4953586 for the gate voltage dependence of the mobility and the redox reaction of capping Al and Ti on LAO/STO.
[25]W. Siemons, G. Koster, H. Yamamoto, W. A. Harrison, G. Lucovsky, T. H. Geballe, D. H. A. Blank, and M. R. Beasley, Phys. Rev. Lett. **98**, 196802 (2007).
[26]Y. Chen, N. Pryds, J. E. Kleibeuker, G. Koster, J. Sun, E. Stamate, B. Shen, G. Rijnders, and S. Linderoth, Nano Lett. **11**, 3774 (2011).
[27]Y. Z. Chen, N. Pryds, J. R. Sun, B. G. Shen, and S. Linderoth, Chin. Phys. B **22**, 116803 (2013).
[28]Y. Z. Chen, F. Trier, T. Wijnands, R. J. Green, N. Gauquelin, R. Egoavil, D. V. Christensen, G. Koster, M. Huijben, N. Bovet, S. Macke, F. He, R. Sutarto, N. H. Andersen, J. a Sulpizio, M. Honig, G. E. D. K. Prawiroatmodjo, T. S. Jespersen, S. Linderoth, S. Ilani, J. Verbeeck, G. Van Tendeloo, G. Rijnders, G. a. Sawatzky, and N. Pryds, Nat. Mater. **14**, 801 (2015).

[29]P. R. Willmott, S. A. Pauli, R. Herger, C. M. Schlepütz, D. Martoccia, B. D. Patterson, B. Delley, R. Clarke, D. Kumah, C. Cionca, and Y. Yacoby, Phys. Rev. Lett. **99**, 155502 (2007).
[30]B.-C. Huang, Y.-P. Chiu, P.-C. Huang, W.-C. Wang, V. T. Tra, J.-C. Yang, Q. He, J.-Y. Lin, C.-S. Chang, and Y.-H. Chu, Phys. Rev. Lett. **109**, 246807 (2012).
[31]G. Singh-Bhalla, C. Bell, J. Ravichandran, W. Siemons, Y. Hikita, S. Salahuddin, A. F. Hebard, H. Y. Hwang, and R. Ramesh, Nat. Phys. **7**, 80 (2011).
[32]J. G. Simmons, J. Appl. Phys. **34**, 238 (1963).
[33]C. H. Du, H. L. Wang, Y. Pu, T. L. Meyer, P. M. Woodward, F. Y. Yang, and P. C. Hammel, Phys. Rev. Lett. **111**, 247202 (2013).